

Diffusion-weighted magnetic resonance imaging for staging liver fibrosis is less reliable in the presence of fat and iron

Robin Bülow · Birger Mensel · Peter Meffert ·
Diego Hernando · Matthias Evert · Jens-Peter Kühn

Received: 30 July 2012 / Revised: 20 September 2012 / Accepted: 10 October 2012 / Published online: 9 November 2012
© European Society of Radiology 2012

Abstract

Objectives To investigate the reliability of diffusion-weighted magnetic resonance imaging (DW-MRI) for staging liver fibrosis in the presence of fat and iron.

Methods Ninety-five patients, including 48 men and 47 women, aged 57.0 ± 14.2 years, underwent liver biopsy. Ninety-six samples were histologically staged for liver fibrosis (0-Ishak score 0; 1-Ishak score 1–4; 2-Ishak score 5–6) and semiquantitatively graded for hepatic iron (0, no; 1, low; 2, moderate; 3, high iron) and for hepatic steatosis. Within 72 h after biopsy, navigator-triggered DW-MRI using b-values of 50/400/800 s/mm^2 was performed in a 1.5-T system, and apparent diffusion coefficients (ADC) were analysed. ADCs were correlated with fibrosis stage, steatosis grade, and iron grade using linear regression.

Results ADC did not correlate with fibrosis stages in either the overall group ($n = 96$; $R^2 = 0.38$; $P = 0.17$) or in the subgroup without liver iron and steatosis ($n = 40$; $R^2 = 0.01$;

$P = 0.75$). ADC decreased significantly with steatosis grade in cases without iron and fibrosis ($n = 42$; $R^2 = 0.28$; $\beta = -5.3$; $P < 0.001$). Liver iron was modestly correlated with ADC in patients without fibrosis and steatosis ($n = 33$; $R^2 = 0.29$; $P = 0.04$), whereas high iron concentrations were associated with low ADC values (group 3: $\beta = -489$; $P = 0.005$; reference: group 0) but intermediate levels were not (group 1/group 2: $P = 0.93/P = 0.54$; reference group: 0).

Conclusions ADC values are confounded by fat and iron. However, even in patients without fat or iron, DW-MRI does not adequately discriminate the stage of fibrosis.

Key Points

- Diffusion-weighted magnetic resonance imaging (DW-MRI) is increasingly used to evaluate liver disease.
- DWI using b-values of 50/400/800 s/mm^2 does not adequately quantify fibrosis.
- Assessment of the apparent diffusion coefficient (ADC) is confounded by fat and iron.
- Fat may influence ADCs by altering water diffusion.
- Iron may influence ADCs by signal decay and noise floor effects.

Keywords Diffusion magnetic resonance imaging · Liver cirrhosis · Iron overload · Fatty liver · Liver diseases

R. Bülow (✉) · B. Mensel · J.-P. Kühn
Department of Radiology and Neuroradiology,
Ernst Moritz Arndt University of Greifswald,
Ferdinand-Sauerbruch-Straße NK,
Greifswald 17475, Germany
e-mail: buelowr@uni-greifswald.de

P. Meffert
Community Medicine,
Ernst Moritz Arndt University of Greifswald,
Walther-Rathenau-Straße 46,
Greifswald 17475, Germany

D. Hernando
Departments of Medical Physics, University of Wisconsin,
1111 Highland Ave,
Madison, WI 53705, USA

M. Evert
Department of Pathology,
Ernst Moritz Arndt University of Greifswald,
Friedrich Loeffler-Strasse 23,
Greifswald 17475, Germany

Introduction

Reversible liver conditions, such as hepatic steatosis and liver iron overload, can progress to liver cirrhosis. Liver cirrhosis is an irreversible disorder for which there is no curative treatment except liver transplant. It may be complicated by portal hypertension, ascites, and clotting dysfunction, finally leading to liver failure and death. Further, subjects with liver cirrhosis have an increased risk of developing primary liver malignancies, especially hepatocellular cancer [1]. Early identification of liver fibrosis, a precursor

to cirrhosis, is necessary to prevent conversion to the irreversible stage.

Liver core biopsy is the reference standard for grading chronic liver disease, including the staging of liver fibrosis. However, liver biopsy is an invasive technique and is associated with complications such as pain and bleeding [2, 3]. Further, liver core biopsy covers only a small part of the liver, and there is the possibility of sampling error [4, 5].

Noninvasive diagnostic investigations for detection of liver fibrosis and cirrhosis are clinically warranted. Ultrasound and computed tomography (CT) can only identify morphological changes of full-blown cirrhosis (enlarged left lateral and caudate lobes, irregular surface, and irregular intrahepatic septa) [6–8]; however, both are limited in grading liver fibrosis. MR elastography may have the potential to assess liver stiffness [9]; however, its clinical role in assessing patients with liver fibrosis remains to be investigated further.

Magnetic resonance imaging (MRI) has the potential to quantify and grade liver fibrosis [10–14]. One promising technique is diffusion-weighted MRI (DW-MRI). This MR technique measures water motion in the extracellular space and water diffusion can be quantified by calculating the apparent diffusion coefficient (ADC). Liver cirrhosis is characterised by the extracellular accumulation of collagen fibres, glycosaminoglycans, and proteoglycans, which theoretically results in restricted water diffusion [12]. DW-MRI may improve the diagnosis of liver fibrosis and cirrhosis, although initial results are contradictory [11, 12, 15–18]. Several investigators have successfully used DW-MRI for assessing hepatic fibrosis and cirrhosis [11, 15, 16]. Two recent studies concluded that DW-MRI is capable of staging liver fibrosis and liver cirrhosis and distinguishing these two conditions from healthy liver tissue [12, 17], whereas another group reported that DW-MRI is limited in differentiating among different fibrosis grades and is only capable of differentiating healthy tissue from cirrhotic liver tissue [18]. Interestingly, different authors have found fundamentally different ADC baseline values in healthy subjects [19–22].

The impact of liver fat on ADC is currently unclear. A recent study found a significant relationship between liver fat and ADC [23], whereas another study found no such relationship [24]. Furthermore, liver iron has been found to have no influence on the ADC value, suggesting that it does not impair quantification of liver cirrhosis [11]. However, in theory and in our clinical experience, there is a signal loss in subjects with liver iron overload because iron shortens the T2/T2* relaxation time [25].

Despite these recent insights, the interpretation of diffusion-weighted images is not well understood in individuals with diffuse liver disease. Contradictory results in previous studies may indicate that DW-MRI is a nonspecific surrogate marker for diffuse liver diseases with liver fat and liver iron as possible confounders. The purpose of our study was to

investigate the reliability of DW-MRI for staging liver fibrosis in the presence of liver fat and liver iron.

Materials and methods

This retrospective study was conducted in accordance with the local Institutional Review Board of Greifswald University Hospital. Written informed consent was obtained separately for liver biopsy and postinterventional MR imaging.

Subjects and study design

Between February 2009 and March 2012, 95 patients underwent a clinically indicated image-guided liver core biopsy. The study population included 48 men and 47 women with a mean age of 57.0 ± 14.2 years. Clinical indications for biopsy were confirmation of suspected focal malignancy in 44 patients and workup of elevated liver enzymes in 51 patients. Samples were obtained using 16–18-gauge biopsy devices. In accordance with our clinical standard, in patients with focal liver lesions, two samples were obtained in one session under image guidance, the first from surrounding nonlesional liver and the second from the target lesion.

Within 24–72 h after liver core biopsy, postinterventional MRI of the upper abdominal organs was performed in each subject, including a chemical-shift-encoded T1-weighted sequence and DW-MRI.

Inclusion criteria for this study were an age of at least 18 years, a valid liver biopsy including a core sample of nonmalignant tissue, and valid histopathological processing of the sample. Subjects with postinterventional haemorrhage were excluded. A haemorrhage was defined as hyperintense signal alterations in the T1-weighted data sets. No subjects had to be excluded because of postinterventional complications.

Overall, 96 valid liver core samples from 95 patients were included in this study. In one patient with geographical fatty degeneration, two samples from nonmalignant tissue in different regions were obtained in the same session.

Histological assessment

One pathologist (M.E.) with more than 14 years of experience in liver pathology reviewed the samples to stage fibrosis using an H&E-stained slide and additionally a Sirius-red-stained slide. The fibrosis stage was determined according to the modified Ishak scale [26]. This scoring system distinguishes three grades: grade 0, no fibrosis (Ishak score 0); grade 1, fibrous expansion (Ishak score 1–4); grade 2, incomplete (marked bridging)/complete cirrhosis (Ishak score 5–6).

Liver fat content was estimated in 5 % steps from 0–100 % including an intermediate step of 3 % using an H&E-stained slide as described in more detail previously [27].

Following the clinical standard, liver iron content was semiquantitatively assessed based on a Perl's Prussian blue reaction using a four-point scoring system: grade 0, no iron; grade 1, low iron; grade 2, moderate iron; grade 3, high iron content.

Postinterventional MR imaging

All postinterventional MRI examinations were performed with a 1.5-T system (Magnetom Avanto, Siemens Healthcare, Erlangen, Germany) using a 12-channel phased-array surface coil.

To obtain anatomical information and to rule out complications after biopsy, a T2*-corrected chemical-shift-encoded multi-echo T1-weighted 3D gradient echo sequence with water-fat separation (TR/TE1/TE2/TE3: 11/2.4/4.8/9.6 ms; flip angle = 10°; bandwidth = ±1,065 Hz/pixel; matrix = 224 × 168 × 64; FOV = 410 × 308 mm; slice thickness: 3 mm) was acquired in each subject.

Thereafter, isotropic diffusion-weighted imaging was performed using a spin-echo-based echo-planar imaging sequence. Imaging series with different diffusion weightings (b-values) were acquired starting with a b-value of 50 mm²/s, followed by two b-values of 400 mm²/s and 800 mm²/s. The acquisition was gated using a prospective acquisition correction technique (PACE). Further imaging parameters were: TR = 1,700 ms; TE = 72 ms; flip angle = 90°; averages = 2; bandwidth = ±1,735 Hz/pixel; matrix: 115 × 192 × 30; FOV phase = 285 mm; parallel imaging acceleration factor = 2; slice thickness = 6 mm. A spectral adiabatic inversion recovery fat saturation technique was used for DW-MRI.

Apparent diffusion coefficient maps (ADC maps) were automatically calculated at the end of each acquisition. ADC calculation was performed using a monoexponential fitting model of the data sets: b50, b400, and b800. The ADC was calculated as follows: $S(b) = S_0 e^{-ADC \cdot b}$.

Image analysis

One reader (R.B.) with more than 2 years of experience in hepatobiliary imaging reviewed the ADC maps using the Osirix software (version 3.8.1, 64 bit, Pixmeo Sarl, Bernex, Switzerland). The observer was unaware of the histopathological results.

A representative liver slice was selected to avoid regions with artefacts and partial volume effects, liver tumours, and large vessels including the central portal vein and the central

hepatic vein. In this slice, the liver was manually segmented, and the mean ADC was documented for each case.

In the one case of geographical fatty degeneration, two independent biopsy samples were obtained—one from the fatty tissue and one from the nonfatty tissue. Two circular ROIs were placed in the liver segments from which biopsies had been obtained.

Statistics

Values were found to be normally distributed. Variables are presented as median values and the corresponding interquartile ranges (IR). Correlation analysis was performed using a linear regression model with robust estimators of the standard errors. First, correlations between ADC and histological fibrosis stage were calculated for all samples independently of the presence of fat and iron. Thereafter, ADC correlations were repeated after exclusion of potential confounders (i.e., liver fat, liver iron, and liver fibrosis) in subgroups, defined as follows:

- ADC versus stage of fibrosis: samples without liver fat and without liver iron;
- ADC versus liver fat: samples without fibrosis/cirrhosis and without iron overload;
- ADC versus liver iron: samples without fibrosis/cirrhosis and without liver fat.

Fat content was treated as a continuous variable. A liver fat content of ≤ 5 % was defined as a sample without liver fat. Liver fibrosis and liver iron load were treated as categorical data.

Calculations were performed using Stata 11.2 (StataCorp 2009. Stata Statistical Software: release 11. College Station, TX: StataCorp LP). All statistical significance tests refer to the linear regression model. Coefficients of the slopes are reported as β-values. The level for statistical significance was set to $P < 0.05$.

Results

In the total study group ($n = 96$), histological fibrosis grades were distributed as follows: no fibrosis (grade 0) in 60 samples, fibrosis expansion (grade 1) in 16 samples, and incomplete/complete cirrhosis (grade 2) in 20 samples. In this group, the median ADC value of $995.0 \times 10^{-3} \text{ mm}^2/\text{s}$ (IR: $849.0 \times 10^{-3} \text{ mm}^2/\text{s} - 1,114.3 \times 10^{-3} \text{ mm}^2/\text{s}$) did not differ significantly between stages of fibrosis or cirrhosis ($P = 0.17$) (Fig. 1a).

ADC versus fibrosis (subgroup analysis)

After exclusion of cases with potential confounders such as liver fat or iron, a subgroup of 40 cases remained: grade 0:

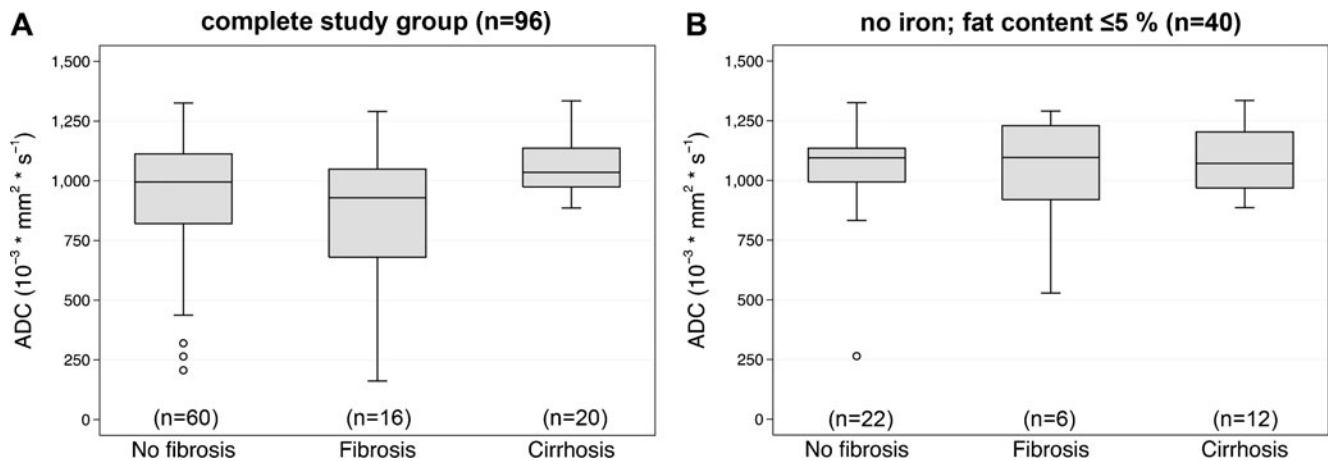


Fig. 1 The *graphs* represent liver ADC values for the three histologically determined grades of liver fibrosis (**a**) for the whole study population and (**b**) for the subgroup without liver iron and with liver fat content $\leq 5\%$. There are no significant differences in median ADC

values among the three fibrosis grades. However, the three fibrosis groups have higher median ADCs and smaller interquartile ranges after exclusion of subjects with liver fat and iron

22 samples; grade 1: 6 samples; grade 2: 12 samples. Analysis within this subgroup also revealed no significant differences in ADC values among fibrosis grades ($P = 0.75$) (Fig. 1b). However, after exclusion of subjects with fat and iron, median ADCs were higher, and variability was smaller.

ADC versus fat (subgroup analysis)

Thereafter samples with liver fibrosis and liver iron were excluded to test the effects of liver fat. This subgroup included 42 samples: 22 samples without liver fat (histological fat content $\leq 5\%$) and 20 samples with liver fat (fat content $> 5\%$). Median histologically determined hepatic fat content was 25% [interquartile range (IR): 15%–45%]. Linear regression of subjects in the subgroup without fibrosis and without liver iron revealed that ADC values decreased significantly with increasing liver fat content ($R^2 = 0.28$; $\beta = -5.3$; $P < 0.001$) (Figs. 2 and 3). In this subgroup, the median ADC of samples without liver fat was $1,012.0 \times 10^{-3} \text{ mm}^2/\text{s}$ (IR: $264.8 \times 10^{-3} \text{ mm}^2/\text{s} - 1,334.7 \times 10^{-3} \text{ mm}^2/\text{s}$) compared to a median ADC of $868.5 \times 10^{-3} \text{ mm}^2/\text{s}$ (IR: $161.7 \times 10^{-3} \text{ mm}^2/\text{s} - 1,268.8 \times 10^{-3} \text{ mm}^2/\text{s}$) in samples with liver fat.

ADC versus iron (subgroup analysis)

The subgroup for analysis of the relationship between ADC and liver iron content in subjects without liver fibrosis/cirrhosis and fat $\leq 5\%$ included 33 samples: 22 samples without iron (grade 0) and 11 samples with an increased liver iron content (grade 1: 5; grade 2: 3; grade 3: 3 samples). Linear regression analysis in this subgroup without fibrosis and without liver fat demonstrated a moderate correlation between ADC values and iron load ($R^2 = 0.29$). However, ADC values in patients with a high iron load

(grade 3) were significantly different from those of patients without liver iron (grade 0) ($\beta = -489$; $P = 0.005$). The median ADC in group 0 (samples without iron) was $1,094.6 \times 10^{-3} \text{ mm}^2/\text{s}$ (IR: $993.7 \times 10^{-3} \text{ mm}^2/\text{s} - 1,134.7 \times 10^{-3} \text{ mm}^2/\text{s}$), whereas the median ADC in samples with high iron content (grade 3) was $506.6 \times 10^{-3} \text{ mm}^2/\text{s}$ (IR: $319.5 \times 10^{-3} \text{ mm}^2/\text{s} - 905.5 \times 10^{-3} \text{ mm}^2/\text{s}$). Only low (group 1) and moderate iron (group 2) levels did not differ significantly from the reference group without liver iron ($P = 0.93$ and $P = 0.54$) (Figs. 2 and 3).

The regression analysis presented in Fig. 3 revealed one sample with a very low ADC of $264.8 \times 10^{-3} \text{ mm}^2/\text{s}$. Liver fat, liver iron, and fibrosis were ruled out by biopsy. The biopsy did not reveal hepatitis in this case (Fig. 3).

Discussion

This study investigated the reliability of DW-MRI for the staging of liver fibrosis and liver cirrhosis in the presence of common liver diseases, specifically fatty liver and liver iron overload. Our results suggest that the DW-MRI technique used in our study has limitations both in staging liver fibrosis and in differentiating between healthy liver and cirrhosis. Furthermore, liver fat and high liver iron levels result in lower ADC and both are possible technical confounders hampering the reliability of DW-MRI independent of the operating mode.

DW-MRI allows sensitive evaluation of the molecular motion of random microscopic molecules, which can be measured by the apparent diffusion coefficient (ADC) [28–30]. This technique is commonly used for the staging of liver fibrosis, evaluation of cirrhosis, quantification of hepatitis, therapy monitoring, and assessment of treatment

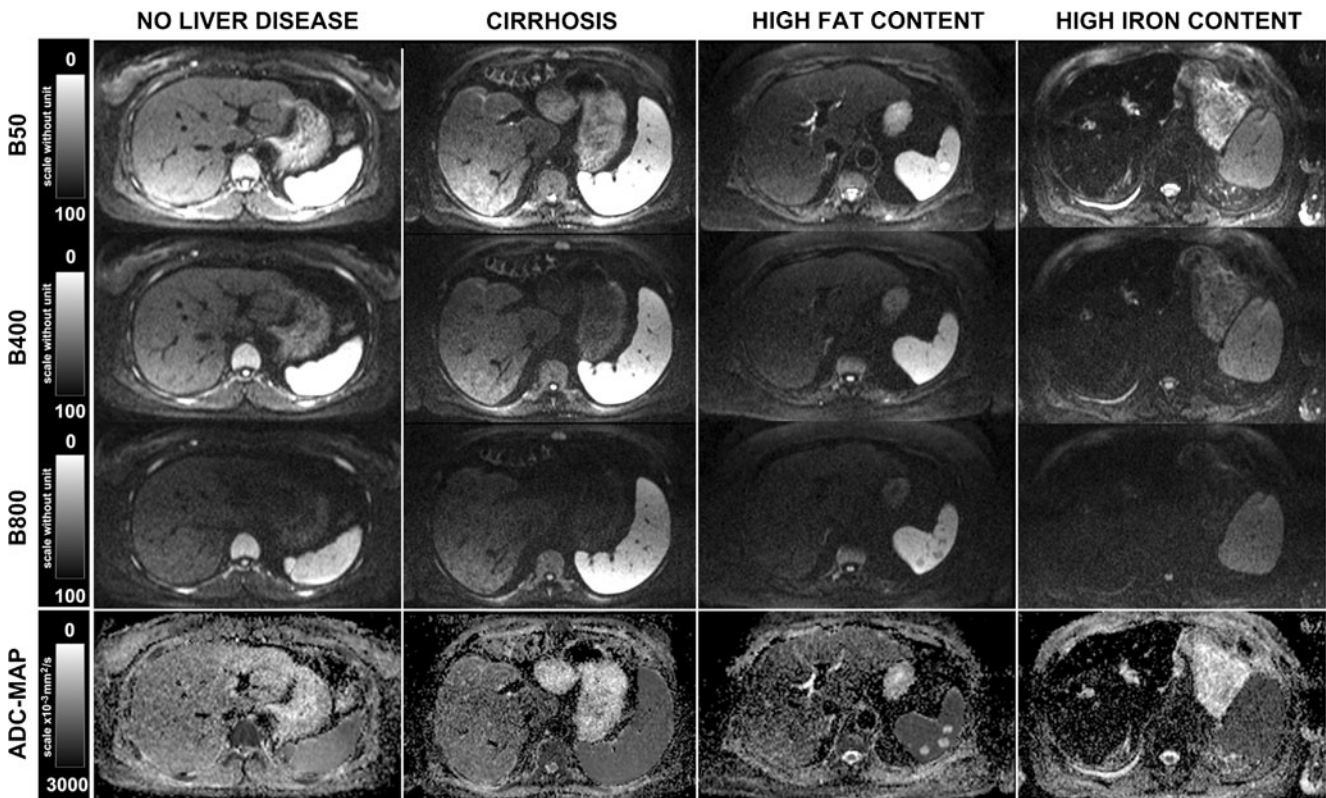


Fig. 2 Comparison of image sets obtained with different diffusion coefficients (50/400/800 mm²/s) and their corresponding ADC maps in clean subgroups of no liver disease, manifest cirrhosis, high liver fat content, and high liver iron content. There was no visually apparent difference in ADC maps between healthy and cirrhotic liver tissue.

However, lower ADC values were calculated in the presence of liver fat and high liver iron content. Furthermore, changes in ADC from iron overload are likely due to signal decay and noise floor effects in subjects with severe iron overload

response [12, 17, 28, 31–33]. Despite the broad spectrum of indications for DW-MRI, our results suggest that the technique is not specific for staging liver fibrosis.

The ADC is affected by several factors, such as permeability and cellular structure [29]. Therefore, both diffusion and perfusion influence the ADC value. At present it is still unclear which effect is more important for the staging of

liver fibrosis. Annet et al. found a correlation of ADC and stage of liver fibrosis in rats, which they no longer observed after the animals had been killed [18]. The authors suggest that the abolished perfusion may explain the decrease of the hepatic ADC measured in vivo in rats with liver fibrosis. To avoid microperfusion effects and to investigate only the impact of true water diffusion, a monoexponential model

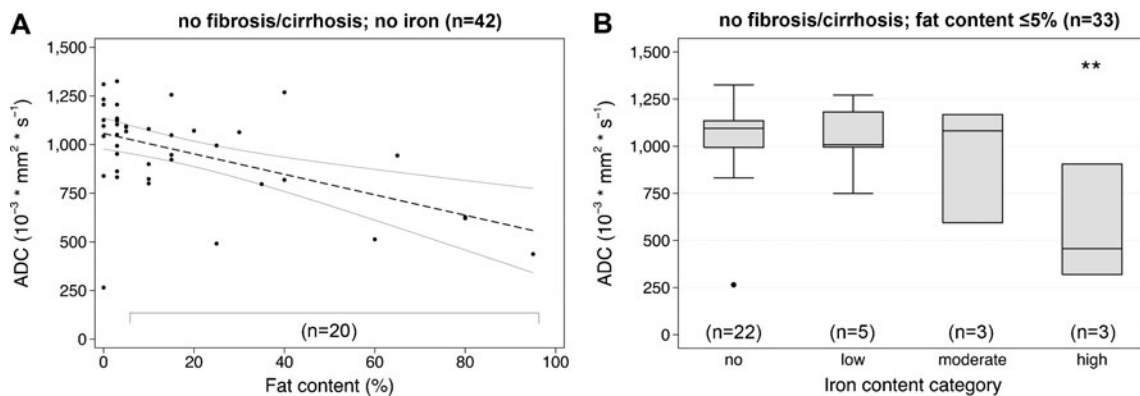


Fig. 3 Linear regression analysis of ADC values for samples without fibrosis/cirrhosis and without liver iron (a) revealed an inverse relationship between ADC and hepatic fat content ($R^2 = 0.28$; $\beta = -5.3$; $P < 0.001$). Furthermore, the median ADC of patients with high iron load

(without fibrosis/and without liver fat) (b) was significantly different (**) from that of patients without liver iron ($\beta = -489$; $P = 0.005$). Therefore, liver fat or high liver iron concentrations affect ADC values, possibly complicating quantitative staging of fibrosis

starting with a b-value of 50 was chosen in this study. Our study identified no relation between ADC values and histopathologically determined stages of fibrosis, suggesting that the molecular water diffusion technique is inadequate for staging liver fibrosis.

In theory, in subjects with liver cirrhosis, arterial and portal venous pressure increases. Additionally, in cirrhosis, intrahepatic and extrahepatic portal venous shunts reduce vascular liver input, leading to decreased microperfusion. First results in humans suggest that microcirculation or perfusion plays a more important role than molecular water diffusion in differentiating cirrhotic from normal livers [34]. Kim et al. used another MR technique for the staging of liver fibrosis—T1-relaxometry before and after oxygen inhalation—in patients with and without liver cirrhosis and concluded that microperfusion is related to the stage of liver fibrosis [10]. Further studies are necessary to assess how microperfusion can be exploited for staging liver fibrosis.

Our findings show that fat affects the ADC of the liver, confirming the results of Poyraz et al. [23]. In theory, liver fat increases the size of hepatocytes. We assume that the increased size of liver cells is associated with a smaller extracellular space. Therefore, molecular motion of water molecules is restricted, and ADC values may be lower than in nonfatty liver. Another possible explanation for the decrease in observed ADC is incomplete fat suppression in fatty livers. Fat suppression in DW-MRI is typically achieved using spectrally selective techniques centered around the water resonance frequency (4.7 ppm). These techniques effectively remove the signal from the main (methylene) fat peak at 1.3 ppm and nearby fat peaks. However, the MR fat signal has a complex spectrum, including several peaks near the water peak (e.g., glycerol and olefinic protons) [35]. These fat peaks are probably not suppressed by spectrally selective techniques and may contribute to the measured DW signal, thus confounding ADC measurement.

The DW-MRI technique is most commonly performed using an echo-planar imaging technique, and it is well known that this technique is prone to susceptibility artefacts [36, 37]. Naganawa et al. reported a signal decay of the raw data in nonmalignant liver tissue after injection of superparamagnetic iron oxide particles: the combination of superparamagnetic iron oxides and DW-MRI significantly improved the detection rate [38]. Our results show a decreased ADC as an expression of the signal decay in the raw data in liver tissue with high iron concentrations. Changes in ADC from high iron overload are likely due to signal decay and noise floor effects in the fitting with severe iron overload. These noise floor effects may influence quantitative ADC analysis.

Furthermore, the ADC we measured in one patient without fibrosis and in the absence of liver iron and liver fat (see outlier in graph 3) suggests that ADC analysis is impaired by at least one additional confounder other than iron and fat.

Our study has several limitations. First, we investigated an inhomogeneous study population including patients with different types of liver lesions and patients on medical treatment, for example. DW-MRI must prove to be robust before it can be used clinically. Further, in this study, biopsy was the gold standard. Liver core biopsy covers only a small region and there is the possibility of a sampling error (e.g., surround lesions), which may limited our study results. Furthermore, diffusion-weighted single-shot echo-planar imaging is limited in terms of image quality, including a poor signal-to-noise ratio, and spatial resolution. This may explain part of the variability observed in ADC measurements observed by us and other investigators. Another limitation is the choice of b-values for DW-MRI and the monoexponential model used for ADC calculation. ADC measurements using a bi-exponential fitting model and a wider range of low (0–50 mm²/s) and high (50–800 mm²/s) b-values would have been better for visualising the effects of microperfusion and real water diffusion separately.

In conclusion, DW-MRI using a monoexponential fitting model and starting with a b-value greater than 50 mm²/s does not seem to discriminate adequately among healthy tissue, fibrosis, and cirrhosis. More studies are necessary to assess DW-MRI using a bi-exponential fitting model and to elucidate the role of microperfusion in the detection and quantification of liver fibrosis and cirrhosis. Biological factors such as hepatic steatosis and high liver iron level were found to influence quantitative ADC assessment. The effects of fat may be due to an actual change in water diffusion or to residual fat signal in fatty livers. Changes in ADC from iron overload are likely due to signal decay and noise floor effects in the fitting with severe iron overload.

Acknowledgments Robin Bülow and Jens-Peter Kühn contributed equally to this work.

Some of subjects were prospectively enrolled in another study: “Kühn JP, Evert M, Friedrich N, et al. (2011) Noninvasive quantification of hepatic fat content using three-echo dixon magnetic resonance imaging with correction for T2* relaxation effects. *Invest Radiol* 46:783-9. PubMed PMID: 21808200”. In this prospective study, we investigated a chemical shift-encoded MRI for liver fat quantification compared to histology. In the present study, retrospective data evaluation was performed to assess liver fibrosis using diffusion-weighted MR imaging.

References

- Colombo M, de Franchis R, Del Ninno E, Sangiovanni A, De Fazio C, Tommasini M, Donato MF, Piva A, Di Carlo V et al (1991) Hepatocellular carcinoma in Italian patients with cirrhosis. *N Engl J Med* 325:675–680
- Thampanitchawong P, Piratvisuth T (1999) Liver biopsy: complications and risk factors. *World J Gastroenterol* 5:301–304

3. Perrault J, McGill DB, Ott BJ, Taylor WF (1978) Liver biopsy: complications in 1000 inpatients and outpatients. *Gastroenterology* 74:103–106
4. Ratziu V, Charlotte F, Heurtier A, Gombert S, Giral P, Bruckert E, Grimaldi A, Capron F, Poynard T et al (2005) Sampling variability of liver biopsy in nonalcoholic fatty liver disease. *Gastroenterology* 128:1898–1906
5. Ratziu V, Bugianesi E, Dixon J, Fassio E, Ekstedt M, Charlotte F, Kechagias S, Poynard T, Olsson R (2007) Histological progression of non-alcoholic fatty liver disease: a critical reassessment based on liver sampling variability. *Aliment Pharmacol Ther* 26:821–830
6. Ong TZ, Tan HJ (2003) Ultrasonography is not reliable in diagnosing liver cirrhosis in clinical practice. *Singap Med J* 44:293–295
7. Di Lelio A, Cestari C, Lomazzi A, Beretta L (1989) Cirrhosis: diagnosis with sonographic study of the liver surface. *Radiology* 172:389–392
8. Brancatelli G, Federle MP, Ambrosini R, Lagalla R, Carriero A, Midiri M, Vilgrain V (2007) Cirrhosis: CT and MR imaging evaluation. *Eur J Radiol* 61:57–69
9. Godfrey EM, Patterson AJ, Priest AN, Davies SE, Joubert I, Krishnan AS, Griffin N, Shaw AS, Alexander GJ et al (2012) A comparison of MR elastography and (31)P MR spectroscopy with histological staging of liver fibrosis. *Eur Radiol*. doi:10.1007/s00330-012-2527-x
10. Kim KA, Park M-S, Kim I-S, Kiefer B, Chung W-S, Kim M-J, Kim KW (2012) Quantitative evaluation of liver cirrhosis using T1 relaxation time with 3 Tesla MRI before and after oxygen inhalation. *J Magn Reson Imaging*. doi:10.1002/jmri.23620
11. Bonekamp S, Torbenson MS, Kamel IR (2011) Diffusion-weighted magnetic resonance imaging for the staging of liver fibrosis. *J Clin Gastroenterol* 45:885–892
12. Bakan AA, Inci E, Bakan S, Gokturk S, Cimilli T (2011) Utility of diffusion-weighted imaging in the evaluation of liver fibrosis. *Eur Radiol* 22:682–687
13. Yin M, Talwalkar JA, Glaser KJ, Manduca A, Grimm RC, Rossman PJ, Fidler JL, Ehman RL (2007) Assessment of hepatic fibrosis with magnetic resonance elastography. *Clin Gastroenterol Hepatol* 5:1207–1213.e2
14. Huwart L, Peeters F, Sinkus R, Annet L, Salameh N, ter Beek LC, Horsmans Y, Van Beers BE (2006) Liver fibrosis: non-invasive assessment with MR elastography. *NMR Biomed* 19:173–179
15. Hu X-F, Liu B, Qian Y-F, Zhang C, Yu Y-Q (2008) A pilot study of hepatic fibrosis with magnetic resonance diffusion-weighted imaging in a rabbit model. *Zhonghua Gan Zang Bing Za Zhi* 16:500–504
16. Zhu N-Y, Chen K-M, Chai W-M, Li W-X, Du L-J (2008) Feasibility of diagnosing and staging liver fibrosis with diffusion weighted imaging. *Chin Med Sci J* 23:183–186
17. Sandrasegaran K, Akisik FM, Lin C, Tahir B, Rajan J, Saxena R, Aisen AM (2009) Value of diffusion-weighted MRI for assessing liver fibrosis and cirrhosis. *Am J Roentgenol* 193:1556–1560. doi:10.2214/AJR.09.2436
18. Annet L, Peeters F, Abarca-Quinones J, Leclercq I, Moulin P, Van Beers BE (2007) Assessment of diffusion-weighted MR imaging in liver fibrosis. *J Magn Reson Imaging* 25:122–128
19. Bruegel M, Holzapfel K, Gaa J, Woertler K, Waldt S, Kiefer B, Stemmer A, Ganter C, Rummeny EJ (2008) Characterization of focal liver lesions by ADC measurements using a respiratory triggered diffusion-weighted single-shot echo-planar MR imaging technique. *Eur Radiol* 18:477–485
20. Namimoto T, Yamashita Y, Sumi S, Tang Y, Takahashi M (1997) Focal liver masses: characterization with diffusion-weighted echoplanar MR imaging. *Radiology* 204:739–744
21. Taouli B, Martin AJ, Qayyum A, Merriman RB, Vigneron D, Yeh BM, Coakley FV (2004) Parallel imaging and diffusion tensor imaging for diffusion-weighted MRI of the liver: preliminary experience in healthy volunteers. *AJR Am J Roentgenol* 183:677–680
22. Do RKG, Chandarana H, Chandanara H, Felker E, Hajdu CH, Babb JS, Kim D, Taouli B (2010) Diagnosis of liver fibrosis and cirrhosis with diffusion-weighted imaging: value of normalized apparent diffusion coefficient using the spleen as reference organ. *Am J Roentgenol* 195:671–676
23. Poyraz AK, Onur MR, Kocakoç E, Oğur E (2011) Diffusion-weighted MRI of fatty liver. *J Magn Reson Imaging*. doi:10.1002/jmri.23519
24. Lee JT, Liau J, Murphy P, Schroeder ME, Sirlin CB, Bydder M (2012) Cross-sectional investigation of correlation between hepatic steatosis and IVIM perfusion on MR imaging. *Magn Reson Imaging* 30:572–578
25. St Pierre TG, Clark PR, Chua-anusorn W, Fleming AJ, Jeffrey GP, Olynyk JK, Pootrakul P, Robins E, Lindeman R (2005) Noninvasive measurement and imaging of liver iron concentrations using proton magnetic resonance. *Blood* 105:855–861
26. Ishak K, Baptista A, Bianchi L, Callea F, De Groote J, Gudat F, Denk H, Desmet V, Korb G et al (1995) Histological grading and staging of chronic hepatitis. *J Hepatol* 22:696–699
27. Kühn JP, Evert M, Friedrich N, Kannengiesser S, Mayerle J, Thiel R, Lerch MM, Dombrowski F, Mensel B et al (2011) Noninvasive quantification of hepatic fat content using three-echo Dixon magnetic resonance imaging with correction for T2* relaxation effects. *Invest Radiol* 46:783–789
28. Soyulu A, Kiliçkesmez O, Poturoğlu S, Dolapçioğlu C, Serez K, Sevindir I, Yaşar N, Akyıldız M, Kumbasar B (2010) Utility of diffusion-weighted MRI for assessing liver fibrosis in patients with chronic active hepatitis. *Diagn Interv Radiol* 16:204–208
29. Le Bihan D (1995) Molecular diffusion, tissue microdynamics and microstructure. *NMR Biomed* 8:375–386
30. Le Bihan D, Tumer R, Douek R, Patronas N (1992) Diffusion MR imaging: clinical applications. *AJR Am J Roentgenol* 159:591–599
31. Kim YK, Lee MW, Lee WJ, Kim SH, Rhim H, Lim JH, Choi D, Kim Y-S, Jang KM et al (2012) Diagnostic accuracy and sensitivity of diffusion-weighted and of gadoteric acid-enhanced 3-T MR imaging alone or in combination in the detection of small liver metastasis (≤ 1.5 cm in diameter). *Invest Radiol* 47:159–166
32. Kenis C, Deckers F, De Foer B, Van Mieghem F, Van Laere S, Pouillon M (2012) Diagnosis of liver metastases: can diffusion-weighted imaging (DWI) be used as a stand alone sequence? *Eur J Radiol* 81:1016–1023
33. Yuan Z, Ye X-D, Dong S, Xu L-C, Xu X-Y, Liu S-Y, Xiao X-S (2010) Role of magnetic resonance diffusion-weighted imaging in evaluating response after chemoembolization of hepatocellular carcinoma. *Eur J Radiol* 75:e9–e14
34. Ichikawa S, Motosugi U, Ichikawa T, Morisaka H, Sano K, Wakayama T, Araki T (2012) Intravoxel incoherent motion imaging of the liver: Which affects more on apparent diffusion coefficient changes of cirrhosis and liver lesions, D or D*? *ISMRM*, 20th ed. Melbourne
35. Hernando D, Karampinos DC, King KF, Haldar JP, Majumdar S, Georgiadis JG, Liang Z-P (2011) Removal of olefinic fat chemical shift artifact in diffusion MRI. *Magn Reson Med* 65:692–701
36. Tonan T, Fujimoto K, Qayyum A, Kawaguchi T, Kawaguchi A, Nakashima O, Okuda K, Hayabuchi N, Sata M (2012) Quantification of hepatic iron concentration in chronic viral hepatitis: usefulness of T2-weighted single-shot spin-echo echo-planar MR imaging. *PLoS One* 7:e33868
37. Qayyum A (2009) Diffusion-weighted imaging in the abdomen and pelvis: concepts and applications. *Radiographics* 29:1797–1810
38. Naganawa S, Sato C, Nakamura T, Kumada H, Ishigaki T, Miura S, Maruyama K, Takizawa O (2005) Diffusion-weighted images of the liver: comparison of tumor detection before and after contrast enhancement with superparamagnetic iron oxide. *J Magn Reson Imaging* 21:836–840